

# Li Ion Diffusivity and Rate Performance of the LiFePO<sub>4</sub> Modified by Cr Doping

Chang Kyoo Park,<sup>†,‡</sup> Sung Bin Park,<sup>†</sup> Ho Chul Shin,<sup>§</sup> Won Il Cho,<sup>‡</sup> and Ho Jang<sup>†,\*</sup>

<sup>†</sup>Department of Materials Science and Engineering, Korea University, Seoul 136-713, Korea. \*E-mail: hojang@korea.ac.kr

<sup>‡</sup>Advanced Battery Center, Korea Institute of Science and Technology 39-1, Hawolgok-dong, Seongbuk-gu, Seoul 136-791, Korea

<sup>§</sup>Energy Materials Lab, R&D center, GS Caltex Corporation 104-4, Munji-dong, Yusung-gu, Daejeon-city 305-380, Korea

Received September 30, 2010, Accepted November 11, 2010

This study reports the root cause of the improved rate performance of LiFePO<sub>4</sub> after Cr doping. By measuring the chemical diffusion coefficient of lithium ( $D_{Li}$ ) using cyclic voltammetry (CV) and electrochemical impedance spectroscopy (EIS), the correlation between the electrochemical performance of LiFePO<sub>4</sub> and Li diffusion is acquired. The diffusion constants for LiFePO<sub>4</sub>/C and LiFe<sub>0.97</sub>Cr<sub>0.03</sub>PO<sub>4</sub>/C measured from CV are  $2.48 \times 10^{-15}$  and  $4.02 \times 10^{-15}$  cm<sup>2</sup> s<sup>-1</sup>, respectively, indicating significant increases in diffusivity after the modification. The difference in diffusivity is also confirmed by EIS and the  $D_{Li}$  values obtained as a function of the lithium content in the cathode. These results suggest that Cr doping facilitates Li ion diffusion during the charge-discharge cycles. The low diffusivity of the LiFePO<sub>4</sub>/C leads to the considerable capacity decline at high discharge rates, while high diffusivity of the LiFe<sub>0.97</sub>Cr<sub>0.03</sub>PO<sub>4</sub>/C maintains the initial capacity, even at high C-rates.

**Key Words:** Lithium iron phosphate, Doping, Chemical diffusion coefficient, Cyclic voltammetry, Electrochemical impedance spectroscopy

## Introduction

Olivine-type lithium iron phosphate (LiFePO<sub>4</sub>) was first proposed by Goodenough's group in 1997,<sup>1</sup> and has attracted considerable attention as a cathode material in lithium-ion batteries for power tools and electric vehicles. This is because LiFePO<sub>4</sub> has many advantages in terms of the theoretical capacity (170 mAh g<sup>-1</sup>), manufacturing cost, thermal stability and toxicity.<sup>2,3</sup> However, its low electronic conductivity ( $10^{-9} \sim 10^{-10}$  S cm<sup>-1</sup>) and low lithium ion diffusivity led to a poor rate capability that has limited its wide commercialization.<sup>4-7</sup> To overcome the shortcomings of LiFePO<sub>4</sub>, considerable research effort has focused on improving the electrical conductivity by coating carbonaceous conductors<sup>8-11</sup> and doping with metallic elements, such as Cr, Mg, Ni or Nb.<sup>12-15</sup>

In particular, lithium diffusion within the particle is a key factor determining the rate performance because it affects the phase transformation between triphylite and heterosite during the charge-discharge cycling of LiFePO<sub>4</sub>. Therefore, an examination of the lithium ion chemical diffusion coefficient,  $D_{Li}$ , was carried out using a range of methods. Prosini *et al.*<sup>16</sup> measured  $D_{Li}$  using a galvanostatic intermittent titration technique (GITT) and electrochemical impedance spectroscopy (EIS), and reported the  $D_{Li}$  value of carbon coated LiFePO<sub>4</sub>/C ranging from  $10^{-17}$  to  $10^{-14}$  cm<sup>2</sup> s<sup>-1</sup>. On the other hand, Yu *et al.*<sup>17</sup> obtained the  $D_{Li}$  value of LiFePO<sub>4</sub>/C using cyclic voltammetry (CV) and reported it to be  $5 \times 10^{-15}$  to  $2.2 \times 10^{-14}$  cm<sup>2</sup> s<sup>-1</sup>. However, there are few reports of the diffusion coefficient by considering super-valent ions doping, despite their importance for examining the detailed mechanism of the electrochemical properties of LiFePO<sub>4</sub> before and after the modifications.

In this study, the diffusion coefficients of carbon coated LiFePO<sub>4</sub>/C and Cr-doped carbon coated LiFe<sub>0.97</sub>Cr<sub>0.03</sub>PO<sub>4</sub>/C were measured by cyclic voltammetry (CV) and electrochemical

impedance spectroscopy (EIS). The mechanism of the performance improvement was examined by comparing the diffusivity of the LiFePO<sub>4</sub> before and after modification.

## Experimental

A mixture of Li<sub>2</sub>CO<sub>3</sub> (Aldrich,  $\geq 99\%$ ), FeC<sub>2</sub>O<sub>4</sub>·2H<sub>2</sub>O (Junsei,  $\geq 99\%$ ), and (NH<sub>4</sub>)H<sub>2</sub>PO<sub>4</sub> (Junsei,  $\geq 99\%$ ) was placed in a zirconia bowl and the mechanochemical reaction was carried out for 3 h using a planetary mill (FRITSCH Pulverisette 5). The rotation speed was 250 rpm and the ball-to-powder weight ratio was 20:1. The resulting powder mixture was heat treated at 750 °C for 10 hours under an Ar + 5% H<sub>2</sub> atmosphere. For the carbon coating and Cr doping, 3 wt % of carbon black powder and 0.01 mol of (CH<sub>3</sub>CO<sub>2</sub>)<sub>2</sub>Cr<sub>3</sub>(OH)<sub>2</sub> were added to the starting materials before mechanochemical activation. The crystal structure of LiFePO<sub>4</sub> was analyzed by X-ray diffraction (XRD; D/MAX-II A) using Cu K $\alpha$  radiation between 15° - 45° (2 $\theta$ ). The morphology of the LiFePO<sub>4</sub> was examined by field emission scanning electron microscopy (FE-SEM, Hitachi, S-4200, Japan).

The cathode of the bare and modified LiFePO<sub>4</sub> was composed of the active material, acetylene black, and polyvinylidene fluoride (PVDF) at a weight ratio of 85:10:5 and coated onto an Al foil. The cathode was held in a vacuum oven at 80 °C for 12 h. After drying, the cathode was 60  $\mu$ m thick and contained approximately 5 - 7 mg cm<sup>-2</sup> of the active materials. The electrolyte was 1 M LiPF<sub>6</sub> in an ethylene carbonate/dimethyl carbonate/ethylmethyl carbonate (EC/DMC/EMC) solution, and lithium foil was used as the counter electrode. A standard coin cell (2032 type) was used to examine the charging and discharging activities of the cathode. The Maccor 4000 battery cyler with cut-off voltages of 2.5 - 4.3 V was used to analyze the rate performance at various C rates. With the exception of the first

5 cycles, which were charged and discharged at 0.1 C, the samples were discharged for five cycles at 0.2, 0.5, 1, 2, 5, 10, 15, 20, 25, and 30 C respectively, and charged at 0.2 C evenly for an accurate comparison of the electrochemical properties between the samples. Cyclic voltammetry (CV) was carried out between 2.8 - 4.2 V at various scan rates from 0.01 to 0.5  $\text{mV s}^{-1}$ . An impedance/gain-phase analyzer (Schlumberger model SI 1260) connected to a Schlumberger model SI 1286 electrochemical interface was used to assess the electrochemical impedance of the cell. The amplitude of the AC signal was 5 mV over the frequency range, 100 kHz and 10 mHz.

## Results and Discussion

The structure of  $\text{LiFePO}_4/\text{C}$  and  $\text{LiFe}_{0.97}\text{Cr}_{0.03}\text{PO}_4/\text{C}$  were analyzed by XRD (Fig. 1). All of them showed a single phase with a typical olivine structure after heat-treatment, suggesting no structural change after the carbon coating and Cr doping.<sup>1</sup> The lattice parameters of the samples were listed in Table 1. It shows that the lattice parameter is slightly decreased after the Cr doping which is attributed to the substitution of  $\text{Cr}^{3+}$  ions with  $\text{Fe}^{2+}$  ions.

Figure 2 shows SEM images of the  $\text{LiFePO}_4/\text{C}$  and  $\text{LiFe}_{0.97}\text{Cr}_{0.03}\text{PO}_4/\text{C}$  samples. The powder was homogeneous and the particle size was within 100 nm diameter. The samples exhibited small adherents to the surface, which appeared to be carbon.

The rate performances of the  $\text{LiFePO}_4/\text{C}$  and  $\text{LiFe}_{0.97}\text{Cr}_{0.03}\text{PO}_4/\text{C}$  were obtained at discharge rates ranging from 0.1 C to 30 C, as shown in Fig. 3. The carbon coating and Cr doping had strong effects on the electrochemical performance of  $\text{LiFePO}_4$ . The initial capacity of the  $\text{LiFePO}_4/\text{C}$  and  $\text{LiFe}_{0.97}\text{Cr}_{0.03}\text{PO}_4/\text{C}$

delivered 152.1  $\text{mAh g}^{-1}$  and 146.5  $\text{mAh g}^{-1}$ , respectively, at the first cycle at 0.1 C, and they exhibited excellent capacity retention until 1 C. However, at 2 C and higher, the capacity of the  $\text{LiFePO}_4/\text{C}$  faded faster than that of Cr doping  $\text{LiFePO}_4/\text{C}$ . While  $\text{LiFe}_{0.97}\text{Cr}_{0.03}\text{PO}_4/\text{C}$  maintained a capacity of 110.8  $\text{mAh g}^{-1}$  at the first cycle at 30 C,  $\text{LiFePO}_4/\text{C}$  delivered only 26.2  $\text{mAh g}^{-1}$  at the same condition. Particularly noteworthy is the improvement in rate performance at high C rates when Cr doping was applied to the  $\text{LiFePO}_4/\text{C}$ . This result substantiates the positive role Cr doping has on the fade resistance of  $\text{LiFePO}_4$ .

The CV profiles from the  $\text{LiFePO}_4/\text{C}$  and  $\text{LiFe}_{0.97}\text{Cr}_{0.03}\text{PO}_4/\text{C}$  were obtained at a scan rate of 0.05  $\text{mV s}^{-1}$  during the redox reaction, as shown in Fig. 4 (a). The figure demonstrates that the redox reaction comprises a two phase system by displaying clear anodic and cathodic peaks, and the shape and intensity of the current peaks are changed considerably by Cr doping. The modified  $\text{LiFe}_{0.97}\text{Cr}_{0.03}\text{PO}_4/\text{C}$  cathode led to reduced peak separation and increased peak currents between the cathodic and anodic peaks compared to  $\text{LiFePO}_4/\text{C}$ , which suggests that the polarization resistance of the cathode had decreased significantly as a result of Cr incorporation.

Cyclic voltammetry of the samples was carried out at different scan rates. Fig. 4 (b) and (c) show the CV profiles of  $\text{LiFePO}_4/\text{C}$  and  $\text{LiFe}_{0.97}\text{Cr}_{0.03}\text{PO}_4/\text{C}$  at scan rate in the range of 0.01 ~ 0.5  $\text{mV s}^{-1}$ , respectively. The peak separation and peak intensity changed as a function of the scan rate. From these profiles, the chemical diffusion coefficient of the Li ion in  $\text{LiFePO}_4$  can be obtained using the Randles-Sevcik equation

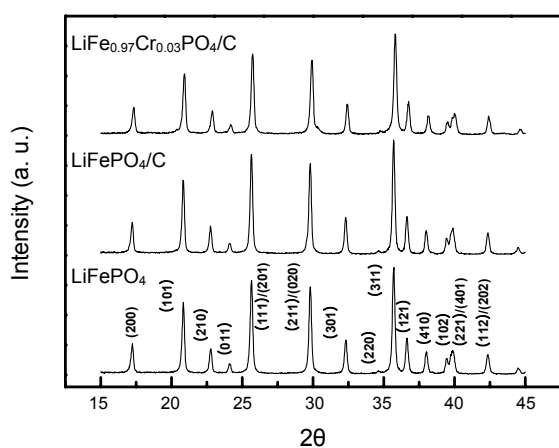


Figure 1. XRD profiles of  $\text{LiFePO}_4$ ,  $\text{LiFePO}_4/\text{C}$ , and  $\text{LiFe}_{0.97}\text{Cr}_{0.03}\text{PO}_4/\text{C}$ .

Table 1. Lattice parameters of  $\text{LiFePO}_4$ ,  $\text{LiFePO}_4/\text{C}$ , and  $\text{LiFe}_{0.97}\text{Cr}_{0.03}\text{PO}_4/\text{C}$

|                                                          | $a$ (Å) | $b$ (Å) | $c$ (Å) | $V$ (Å <sup>3</sup> ) |
|----------------------------------------------------------|---------|---------|---------|-----------------------|
| $\text{LiFePO}_4$                                        | 10.2919 | 5.9908  | 4.6782  | 288.4452              |
| $\text{LiFePO}_4/\text{C}$                               | 10.2998 | 5.9894  | 4.6778  | 288.5691              |
| $\text{LiFe}_{0.97}\text{Cr}_{0.03}\text{PO}_4/\text{C}$ | 10.2603 | 5.9692  | 4.6690  | 285.9568              |

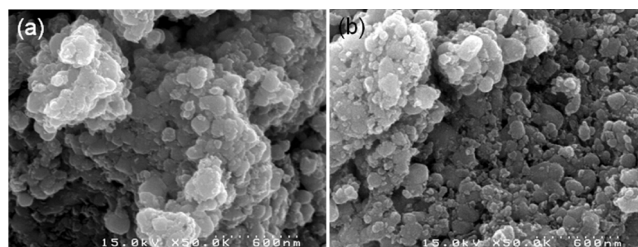


Figure 2. SEM micrographs of (a) carbon-coated and (b) carbon-coated and Cr-doped  $\text{LiFePO}_4$ .

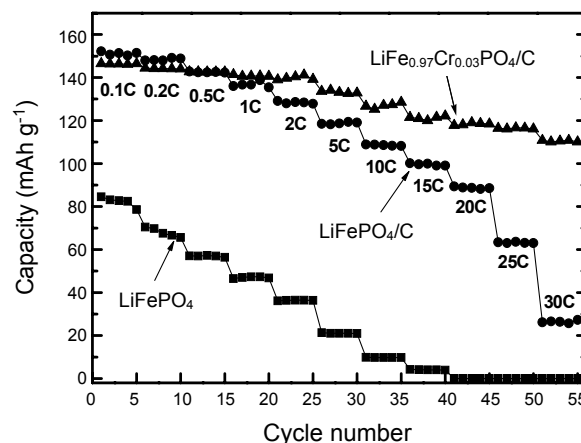
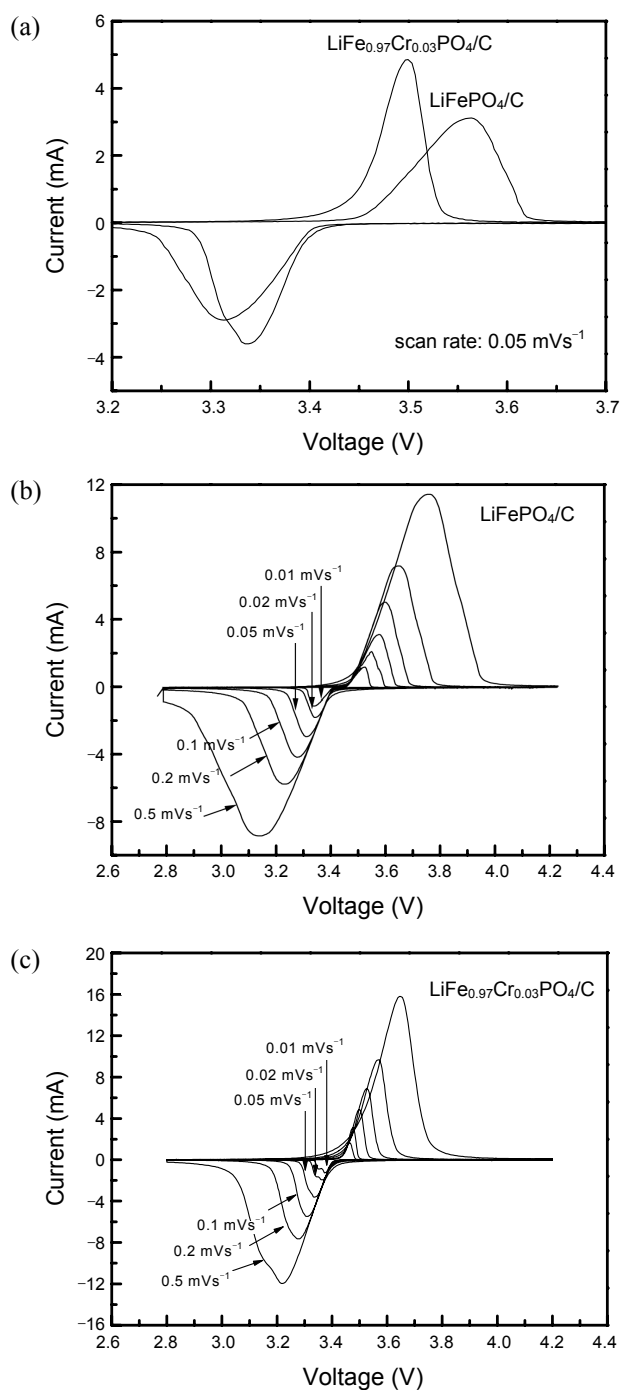


Figure 3. Rate performances of  $\text{LiFePO}_4$ ,  $\text{LiFePO}_4/\text{C}$ , and  $\text{LiFe}_{0.97}\text{Cr}_{0.03}\text{PO}_4/\text{C}$  during discharging at various C rates.



**Figure 4.** CV profiles of (a) the LiFePO<sub>4</sub>/C and LiFe<sub>0.97</sub>Cr<sub>0.03</sub>PO<sub>4</sub>/C at a scan rate of 0.05 mV s<sup>-1</sup> and (b) the LiFePO<sub>4</sub>/C and (c) the LiFe<sub>0.97</sub>Cr<sub>0.03</sub>PO<sub>4</sub>/C with different scan rates.

(Eq. 1), which describes the relationship between the peak current ( $i_p$ ) and square root of the scan rate ( $V^{1/2}$ ).<sup>19</sup>

$$I_p/m = 0.4463F(F/RT)^{1/2}C_{Li}V^{1/2}AD^{1/2} \quad (1)$$

where  $I_p$  is the peak current in amperes,  $m$  is the mass of electrode,  $F$  is the Faraday constant,  $C_{Li}$  is the initial concentration of Li in mol/cm<sup>3</sup>,  $V$  is scan rate in V/s,  $A$  is electrode area in cm<sup>2</sup> and  $D$  is the diffusion constant in cm<sup>2</sup>/s. In the case of

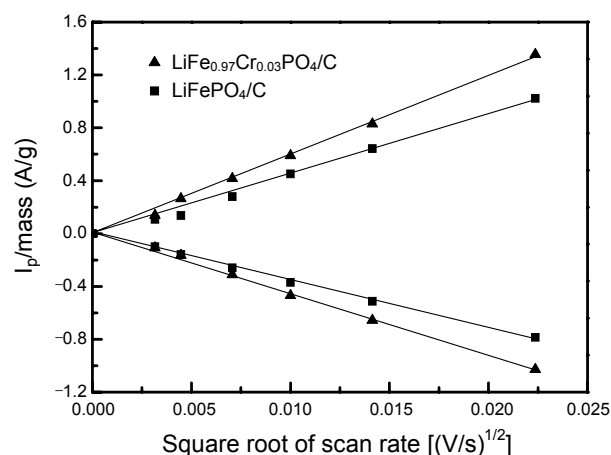


**Figure 5.** Graph of the LiFePO<sub>4</sub>/C and LiFe<sub>0.97</sub>Cr<sub>0.03</sub>PO<sub>4</sub>/C with normalized peak current and square root of the scan rate.

**Table 2.** Chemical diffusion constants of LiFePO<sub>4</sub>/C and LiFe<sub>0.97</sub>Cr<sub>0.03</sub>PO<sub>4</sub>/C obtained from CV

| Cathode materials                             | LiFePO <sub>4</sub> /C | LiFe <sub>0.97</sub> Cr <sub>0.03</sub> PO <sub>4</sub> /C |
|-----------------------------------------------|------------------------|------------------------------------------------------------|
| Anodic D (cm <sup>2</sup> s <sup>-1</sup> )   | $4.39 \times 10^{-15}$ | $6.73 \times 10^{-15}$                                     |
| Cathodic D (cm <sup>2</sup> s <sup>-1</sup> ) | $2.48 \times 10^{-15}$ | $4.02 \times 10^{-15}$                                     |

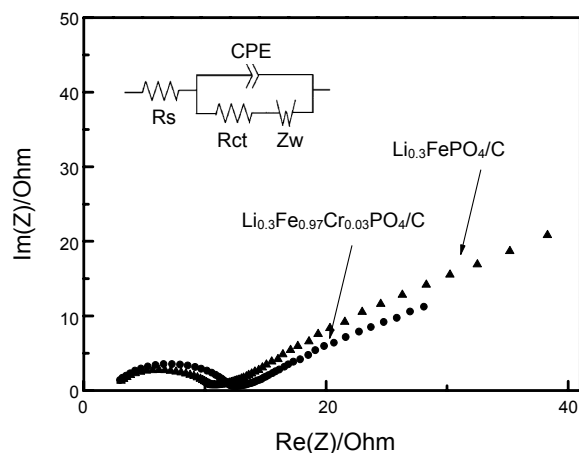


**Figure 6.** The equivalent circuit and impedance spectra of the cells for lithium content at 30%. Frequency range: 0.01 Hz - 100 kHz.

LiFePO<sub>4</sub>, Li ions were inserted and extracted along the [010] direction through the (010) plane.<sup>20,21</sup> Therefore, one-third of the total Brunauer-Emmett-Teller (BET) surface area was used as parameter A in Eq. 1 instead of the entire electrode area.<sup>17</sup> Fig. 5 shows a plot of  $I_p/m$  as a function of the square root of the scan rate ( $V^{1/2}$ ) in the case of LiFePO<sub>4</sub>/C and LiFe<sub>0.97</sub>Cr<sub>0.03</sub>PO<sub>4</sub>/C to calculate the diffusion constants, as listed in Table 2. The cathodic diffusion constant increased approximately 62% after Cr doping on the LiFePO<sub>4</sub>/C. The chemical diffusion coefficients obtained in this study are consistent with those measured by Yu *et al.*<sup>17</sup> and Kumar *et al.*<sup>18</sup> using CV.

The effects of the metal doping on the rate performance of the LiFePO<sub>4</sub> cathodes were also examined by EIS at various lithium contents in the cathode during discharging. Before each

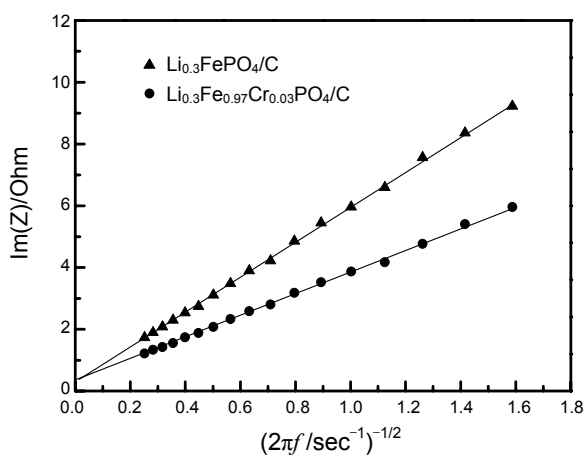


**Figure 7.** The relationship between imaginary resistance and inverse square root of angular speed for  $\text{Li}_{0.3}\text{FePO}_4/\text{C}$  and  $\text{Li}_{0.3}\text{Fe}_{0.97}\text{Cr}_{0.03}\text{PO}_4/\text{C}$ .

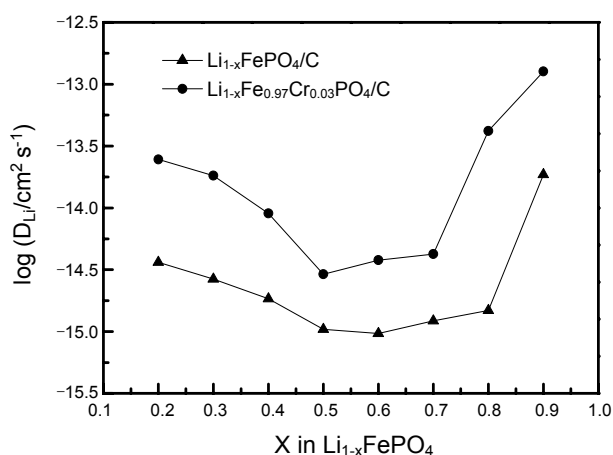


**Figure 8.** Chemical diffusion coefficients of Li in  $\text{Li}_{1-x}\text{FePO}_4$  at various Li contents (EIS).

EIS measurement, several preliminary galvanostatic cycles were performed for stable SEI film formation and the good permeation of the electrolyte into the active material. Fig. 6 shows an equivalent circuit and Nyquist plots of the samples at Li content of 30% in  $\text{LiFePO}_4$ .  $R_s$  represents the Ohmic resistance between the electrolyte and electrode, which corresponds to the starting point of the semicircle in the high frequency region. In addition, the  $R_{ct}$  expresses the charge transfer resistance, which illustrates the radius of the semicircle in a medium frequency region. The inclined line, which was fitted to a straight line with a slope of  $45^\circ$  in the spectrum in the low frequency region, indicates the Warburg impedance  $Z_w$ , which is related to Li ion diffusion within the  $\text{LiFePO}_4$  particle. The model proposed by Ho *et al.*<sup>22</sup> was used to determine the diffusion coefficients of the bare and modified  $\text{LiFePO}_4$ , as described in Eq. 2.

$$D_{\text{Li}} = 1/2 [(V_M/SFA)(\delta E/\delta X)]^2 \quad (2)$$

where  $V_M$  is the molar volume of the  $\text{LiFePO}_4$ ,  $S$  is the surface area of the cathode,  $F$  is the Faraday constant,  $\delta E/\delta X$  is the slope of the coulometric titration curve, and  $A$  is obtained from the Warburg impedance. Fig. 7 shows the relationship between

the imaginary resistance ( $\text{Im}(Z)$ ) and the inverse square root of angular speed ( $(2\pi f)^{-1/2}$ ) in the low frequency range for the  $\text{LiFePO}_4$  when Li content is 30%. The slopes of these plots were substituted in Eq. 3 to determine the diffusion coefficient of lithium at different  $x$  values in the  $\text{Li}_{1-x}\text{FePO}_4$  cathodes. Fig. 8 shows the diffusion coefficients of Li ions obtained from the EIS method. The figure suggests that Cr doping on  $\text{LiFePO}_4$  was effective in improving chemical diffusion of Li ion in the particle. When the Li content in  $\text{LiFePO}_4$  was 30%, the diffusion coefficient of  $\text{Li}_{0.3}\text{Fe}_{0.97}\text{Cr}_{0.03}\text{PO}_4/\text{C}$  was approximately 3.5 times higher than that of  $\text{Li}_{0.3}\text{FePO}_4/\text{C}$ . The diffusion coefficient of the  $\text{LiFePO}_4/\text{C}$  is well consistent with the diffusion data obtained from Prosini *et al.*<sup>16</sup> and Zhu *et al.*<sup>23</sup>

The diffusion constant obtained from CV and EIS indicated  $\text{LiFe}_{0.97}\text{Cr}_{0.03}\text{PO}_4/\text{C}$  have higher  $D_{\text{Li}}$  value than that of  $\text{LiFePO}_4/\text{C}$ . The considerable improvement in chemical diffusion coefficient suggests that the Cr doping directly affected  $D_{\text{Li}}$  in the particle which lead to enhance the rate performance. The improvement in rate performance by Cr doping was attributed to the structural changes in the  $\text{LiFePO}_4$ . Cr doping increases the concentration of ionic vacancies<sup>24</sup> with accompanying conduction electrons to maintain neutrality of the lattice in  $\text{LiFePO}_4$ .<sup>25</sup> It facilitates the Li ion diffusivity which increases the kinetics of the phase transformation between heterosite (charged phase) and triphylite (discharged phase) during the charge-discharge cycles.<sup>26</sup>

## Conclusions

The chemical diffusion coefficients of  $\text{LiFePO}_4/\text{C}$  and  $\text{LiFe}_{0.97}\text{Cr}_{0.03}\text{PO}_4/\text{C}$  were measured using CV and EIS techniques to find the cause of the improvement in rate performance after the modification. CV analysis revealed an approximately 62% increase in diffusion constant was achieved by complementary Cr doping. The diffusion constants measured from EIS also showed consistent results with CV result that the Li diffusivity of  $\text{LiFe}_{0.97}\text{Cr}_{0.03}\text{PO}_4/\text{C}$  was considerably higher than that of  $\text{LiFePO}_4/\text{C}$ . The measured rate performance also confirmed that the higher diffusion constants were the root cause of the improvement of the electrochemical performance of the modified  $\text{LiFePO}_4/\text{C}$ .

**Acknowledgments.** This work was supported by Energy Resource R&D Programs (2009201010003B-11-3-020 and 2008EEL11P0800002009) under the Ministry of Knowledge Economy, Republic of Korea.

## References

1. Padhi, A. K.; Nanjundaswamy, K. S.; Goodenough, J. B. *J. Electrochem. Soc.* **1997**, *144*, 1188.
2. MacNeil, D. D.; Lu, Z.; Chen, Z.; Dahn, J. R. *J. Power Sources*. **2002**, *108*, 8.
3. Takahashi, M.; Tobishima, S. I.; Takei, K.; Sakurai, Y. *Solid State Ionics* **2002**, *148*, 283.
4. Padhi, A. K.; Nanjundaswamy, K. S.; Masquelier, C.; Okada, S.; Goodenough, J. B. *J. Electrochem. Soc.* **1997**, *144*, 1609.
5. Takahashi, M.; Tobishima, S.; Takei, K.; Sakurai, Y. *J. Power Sources* **2001**, *97/98*, 508.

6. Barker, J.; Saidi, M. Y.; Swoyer, J. L. *Electrochem. Solid-State Lett.* **2003**, *6*, A53.
  7. Andersson, A. S.; Kalska, B.; Haggstrom, L.; Thomas, J. O. *Solid State Ionics* **2000**, *130*, 41.
  8. Ravet, N.; Chouinard, Y.; Magnan, J. F.; Besner, S.; Gauthier, M.; Armand, M. *J. Power Sources* **2001**, *97-98*, 503.
  9. Prosini, P. P.; Zane, D.; Pasquali, M. *Electrochim. Acta* **2001**, *46*, 3517.
  10. Huang, H.; Yin, S. C.; Nazar, L. F. *Electrochem. Solid State Lett.* **2001**, *4*, A170.
  11. Chen, Z.; Dahn, J. R. *J. Electrochem. Soc.* **2002**, *149*, A1184.
  12. Chung, S. Y.; Bloking, J. T.; Chiang, Y. M. *Nat. Mater.* **2002**, *1*, 123.
  13. Shi, S.; Liu, L.; Ouyang, C.; Wang, D. S.; Wang, Z.; Chen, L.; Huang, X. *Phys. Rev. B* **2003**, *68*, 1.
  14. Wang, D.; Li, H.; Shi, S.; Huang, X.; Chen, L. *Electrochim. Acta* **2005**, *50*, 2955.
  15. Wang, G. X.; Bewlay, S.; Needham, S. A. *J. Electrochem. Soc.* **2006**, *153*, A25.
  16. Prosini, P. P.; Lisi, M.; Zane, D.; Pasquali, M. *Solid State Ionics* **2002**, *148*, 45.
  17. Yu, D. Y. W.; Fietzek, C.; Weydanz, W.; Donoue, K. *J. Electrochem. Soc.* **2007**, *154*, A253.
  18. Kumar, A.; Thomas, R.; Karan, N. K.; Saavedra-Arias, J. J. *J. Nanotechnology* **2009**, *2009*, 10.
  19. Bard, A. J.; Faulkner, L. R. *Electrochemical Methods*; John Wiley & Sons, Inc.: New York, 1980.
  20. Morgan, D.; Van der Ven, A.; Cedar, G. *Electrochem. Solid-State Lett.* **2004**, *7*, A30.
  21. Ouyang, C.; Shi, S.; Wang, Z.; Huang, X.; Chen, L. *Phys. Rev. B* **2004**, *69*, 1.
  22. Ho, C.; Raistrick, I. D.; Huggins, R. A. *J. Electrochem. Soc.* **1980**, *127*, 343.
  23. Zhu, Y.; Wang, C. *J. Phys. Chem. C* **2010**, *114*, 2830.
  24. Meethong, N.; Kao, Y. h.; Speakman, S. A.; Chiang, Y. M. *Adv. Funct. Mater.* **2009**, *19*, 1060.
  25. Jaffe, K. *Oxidation of Metals*; Plenum Press: 1965.
  26. Shin, H. C.; Park, S. B.; Jang, H. *Electrochim. Acta* **2008**, *53*, 7946.
-